Coules, H. E., & Horne, G. (2019). Effects of residual stress and localised strain-hardening on the fracture of ductile materials. In *Procedia Structural Integrity* (Vol. 17 (2019), pp. 934-941)
https://doi.org/10.1016/j.prostr.2019.08.124

Available online at www.sciencedirect.com

ScienceDirect

Procedia Structural Integrity 17 (2019) 934–941

Structural Integrity Procedia

www.elsevier.com/locate/procedia

ICSI 2019 The 3rd International Conference on Structural Integrity

Effects of residual stresses and localised strain-hardening on the fracture of ductile materials

H. E Coules* and G. C. M. Horne

Department of Mechnaical Engineering, University of Bristol, University Walk, Bristol, BS8 1TR, UK

Abstract

The strain history of a ductile material can affect its apparent initiation fracture toughness as well as its resistance to subsequent crack growth. Using neutron diffraction or synchrotron X-ray diffraction in conjunction with digital image correlation, it is possible to map both the total strain around the tip of a propagating crack, and the elastic strain component. Separating the elastic and irreversible strain components allows us to experimentally investigate the effects that residual stresses and prior strain-hardening have on crack propagation. This article presents the results of two experiments using these techniques. In the first experiment, it was shown that residual stresses in a 7xxx-series aluminium alloy affect not only the initiation of fracture but also fracture propagation. During crack propagation, residual stress relaxation occurs due to extension of the crack and plastic deformation in the region ahead of the crack tip. This affects the material's apparent crack growth resistance in a non-linear manner and hence changes its fracture stability. In a second experiment, it was shown that the plastic zone ahead of a crack in a ductile material (in this case a ductile ferritic steel) can be modified by localised strain-hardening prior to fracture. Localised strain-hardening using an indentation tool was observed to cause small increases in the specimens' peak load capacity and its energy absorption prior to the onset of unstable tearing. Using synchrotron diffraction, it was shown that is because hardening a region ahead of the crack tip causes stress redistribution to this region and away from the crack tip itself during fracture loading. These findings can inform how ductile and semi-ductile fracture is treated in structural integrity assessment procedures, particularly in the presence of residual stress. They also suggest that new localised peening treatments to improve the fracture resistance of structures in certain areas may be possible.

Peer-review under responsibility of the ICSI 2019 organizers.

Keywords: Ductile fracture; Plasticity; Residual stress; Strain Energy Release Rate

* Corresponding author. Tel.:+44 (0)117 3315946; Email: harry.coules@bristol.ac.uk

2452-3216
Peer-review under responsibility of the ICSI 2019 organizers.
10.1016/j.prostr.2019.08.124

Nomenclature

CMOD	Crack Mouth Opening Displacement
C(T)	Compact (Tension) fracture specimen
DIC	Digital Image Correlation
FEA	Finite Element Analysis
LEFM	Linear Elastic Fracture Mechanics
SALSA	Strain Analyser for Large- and Small-scale Applications (neutron diffractometer)
SERR	Strain Energy Release Rate
SIF	Stress Intensity Factor

1. Introduction

In brittle and semi-brittle materials, the process of fracture initiation from a pre-existing flaw or crack-like defect is controlled by the crack tip loading. In Linear Elastic Fracture Mechanics (LEFM) this can be characterised using the crack tip Stress Intensity Factor (SIF), denoted K_I. In materials and components which are subject to complex loads, superposition of crack tip loading from multiple sources (such as residual, thermal and externally-applied stresses) can occur. In ductile and semi-ductile materials, including most metals, significant plasticity may occur at the crack tip prior to fracture initiation. Therefore the effect that the plastic interaction between loading modes has on the initiation of fracture must be taken into account in structural integrity assessment (Budden & Sharples 2003). Commonly-used structural integrity assessment procedures such as the British Standard BS 7910 (BSi 2013) and the R6 code used by the UK nuclear industry (EDF 2015) include approximate methods for quantifying the plasticity interaction between 'primary' (i.e. applied) and 'secondary' (i.e. thermal or residual) loading.

Although the effect of secondary stresses on non-brittle fracture initiation can often be difficult to calculate for any specific case, the general principles are now relatively well-understood. In summary, plasticity effects occurring prior to fracture initiation mean that residual and applied stresses do not superimpose linearly (Withers 2007). Less clear are the effects that secondary stresses have on the *propagation* of cracks in ductile materials after fracture has initiated. Likewise, residual stresses are often associated with non-uniform distributions of material strain hardening since they are a result of strain incompatibility typically introduced via non-uniform plastic deformation. The effects of these variations in strain-hardening state on subsequent fracture is thought to be significant but has not been investigated rigorously. One way to take these factors onto account when Finite Element Analysis (FEA) is used to determine the Strain Energy Release Rate (SERR) is via the use of a modified form of the J-integral, which was proposed for thermal stresses by Wilson & Yu (Wilson & Yu 1979) and extended to the case of residual stress by Lei (Lei 2005). This can be expressed as:

$$J_{mod} = \int_{\Gamma} \left(W\delta_{1j} - \sigma_{ij}u_{i,1}\right)n_j \, ds + \int_{A} \sigma_{ij}\varepsilon^{0}_{ij,1} \, dA \tag{1}$$

where J_{mod} is the modified J-integral, W is the strain energy density, u_i is the displacement, σ_{ij} is the stress tensor and ε^{0}_{ij} is an initial strain tensor. Γ is a closed contour surrounding the crack tip, for which A is the enclosed area, s is the path length, and n_j is an outward-facing normal vector. δ_{ij} is the Kronecker delta. This modified J-integral value can then be used to predict the initiation of ductile fracture.

This article describes a pair of linked investigations into the fracture behavior of non-brittle materials containing residual stresses and distributions of prior strain-hardening. The first experiment concerns the effect that residual stress has on crack propagation in a non-brittle material, and was used to show that Lei's modified J-integral formulation (Equation 1) can be used to predict of both fracture initiation and crack propagation in a residually-

stressed material. The second experiment showed that the modified J-integral formulation can also be applied to ductile tearing, and that for ductile tearing the prior strain-hardening state of material close to the crack tip can play a significant role in tearing initiation. In both experiments, radiation scattering methods (specifically neutron and synchrotron X-ray diffraction) were used to characterise the elastic field around crack tips as they were loaded in situ, which Digital Image Correlation (DIC) was simultaneously used to determine the total strain over the specimens' surface.

2. Experiments

2.1. Effects of residual stress on fracture propagation

In this experiment, Compact Tension (C(T)) fracture specimens of aluminium alloy 7475-T7351 were loaded to failure while measuring the applied load and Crack Mouth Opening Displacement (CMOD) (Coules et al. 2018). They were interrupted at several points to enable mapping of the elastic strain field around the crack tip using angle-dispersive neutron diffraction and the entire experiment was performed on the SALSA beamline at the Institut Laue-Langevin, France. Two types of specimens were compared: plain specimens of as-received material, and specimens which had a residual stress field introduced ahead of the crack tip by indenting the specimen using a pair of opposed cylindrical indenters of EN24 tool steel. This indentation was performed prior to the experiment and using a force of 75 kN. A diagram of the specimen geometry is shown in Figure 1a; the specimens were fatigue pre-cracked in accordance with ASTM E561-15a (ASTM 2015). Both side-grooved (to allow within-standard fracture toughness measurements) and non-side-grooved (to allow surface DIC measurements) fracture specimens were used.

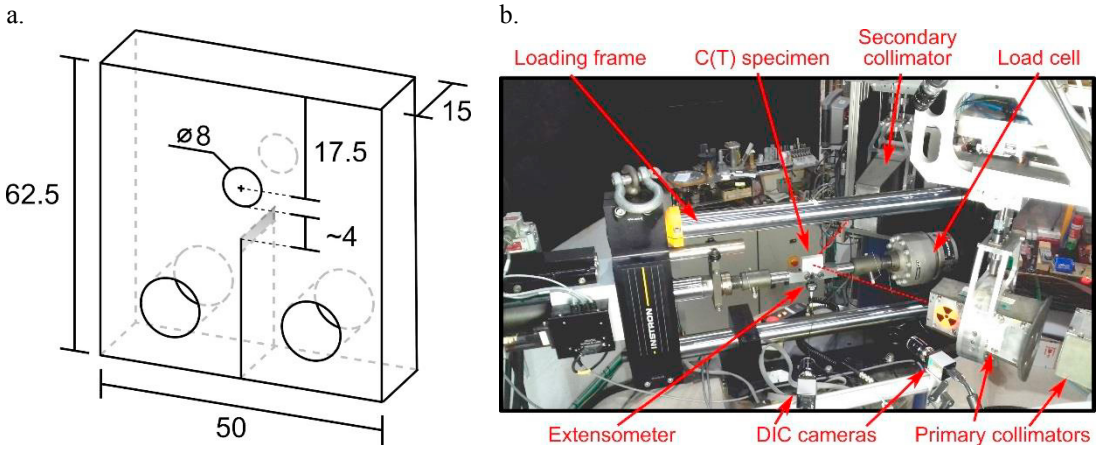

Figure 1: a.) Geometry of AA 7475-T7351 fracture test specimens (dimensions in mm). b.) SALSA neutron diffractometer with specimen and loading rig *in situ*. All diffraction measurements were taken at the specimen's mid-thickness plane.

Using the load vs. CMOD measurements, the fracture resistance curves (K_R curve) for both indented and non-indented types of specimen were determined. These are shown in Figure 2. In the indented specimens, fracture initiates at a lower level of crack tip stress intensity factor, and the fracture also propagates more easily through the material – i.e. the K_R curve remains lower. Figure 3 shows the elastic strain at the mid-thickness plane of the specimens during fracture testing. The indented specimen contains a clearly visible elastic strain distribution prior to loading, indicating the presence of a residual stress. This causes positive Mode I (i.e. opening-mode) loading of the crack, which then superimposes with the Mode I loading caused by the applied load. It was observed the superposition of the residual and applied stress fields at the crack tip was not strictly additive even in the stages of loading prior to crack propagation, i.e. material non-linearity occurs prior to fracture initiation.

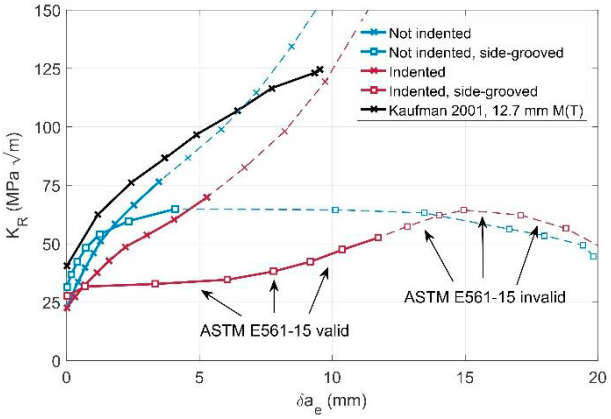

Figure 2: Fracture resistance curves for 15 mm thick C(T) specimens of AA 7475-T7351 with and without side-grooves and indentations causing residual stress. Note the use of effective crack length on the horizontal axis.

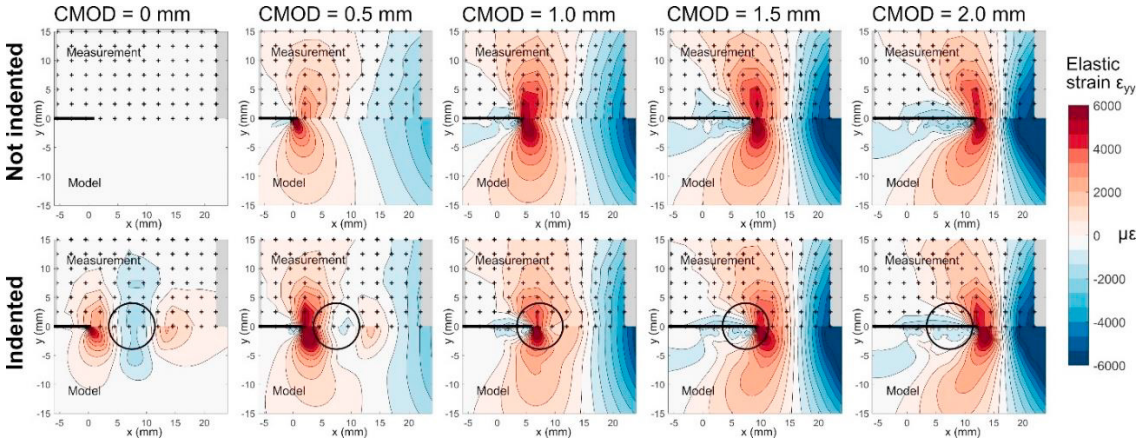

Figure 3: Crack tip elastic strain fields (crack transverse ε_{yy} component pictured) during fracture loading of indented and non-indented specimens. Each sub-image compares results from neutron diffraction measurement with FE predictions. The crack grows from left to right and a circle indicates the indented zone. Note the presence of residual elastic strain in the indented specimen prior to loading (CMOD = 0 mm).

FEA of the loading process was performed and validated using the neutron diffraction results (Figure 3). The FEA results for residual-stress-bearing fracture specimens (see Figure 4) confirmed that material plasticity occurs both prior to and during crack propagation. From the FE model, the observed differences in plastic zone development in the indented specimens with respect to non-indented ones were shown to be caused by a combination of the residual stress and prior strain hardening. The specimens' initial differences in apparent fracture resistance are caused by the initial opening-mode residual stress in the indented test piece. However, as the crack propagates in the indented specimen, prior strain hardening suppresses crack tip plasticity as the crack tip moves through the indented region. This reduces the material's apparent fracture resistance until the crack propagates to the far side of the indented zone. Due to these plasticity effects, the observed differences in the apparent fracture propagation resistance (Figure 2) between indented and non-indented specimens cannot be accounted for using elastic superposition of the residual stress and applied stress fields, as was performed by previous work by Hill and Van Dalen (Hill & VanDalen 2008). Instead, using the modified J-integral formulation (Equation 1) to calculate the elastic-plastic SERR, taking into account initial stresses and strains introduced by indentation, brought the material fracture resistance results for both types of specimen into agreement. This implies that the modified J-integral formulation is a reasonably accurate predictor of the SERR, during both fracture initiation and crack propagation in elastic-plastic materials.

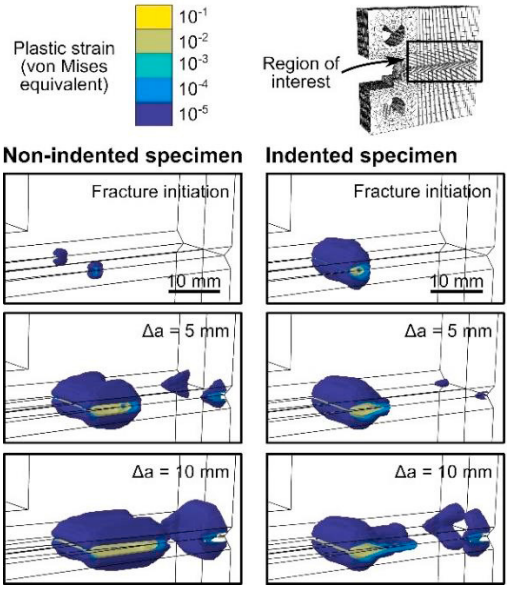

Figure 4: FEA predictions of plastic zone development around the tip of propagating cracks in C(T) specimens in 7475-T7341 aluminium alloy specimens with and without indentation ahead of the initial crack tip.

2.2. Non-uniform strain hardening distributions

A second experiment considered ductile tearing and whether the strain energy dissipation in a ductile material can be influenced by distributions of prior strain-hardening to the extent that the apparent tearing resistance of the material can be modified. As with the experiment described in Section 2.1, C(T) specimens with and without indentation ahead of the crack tip were loaded monotonically to failure, and diffraction methods and DIC were used to observe the crack tip stress and strain fields at several steps during loading. However, in this case thin (5 mm thickness) specimens of a ductile ferritic pressure vessel steel (BS 1501-224 28B) were studied, and energy-dispersive synchrotron X-ray diffraction was used to measure the crack tip stresses (Coules et al. 2019). The experiment was performed on the I12 beamline at Diamond Light Source, Oxfordshire, UK (Drakopoulos et al. 2015), in the configuration shown in Figure 5. As before, DIC measurements were used to map the surface strains as indented and non-indented specimens were loaded to failure, and a FE model of the indentation and loading processes was developed.

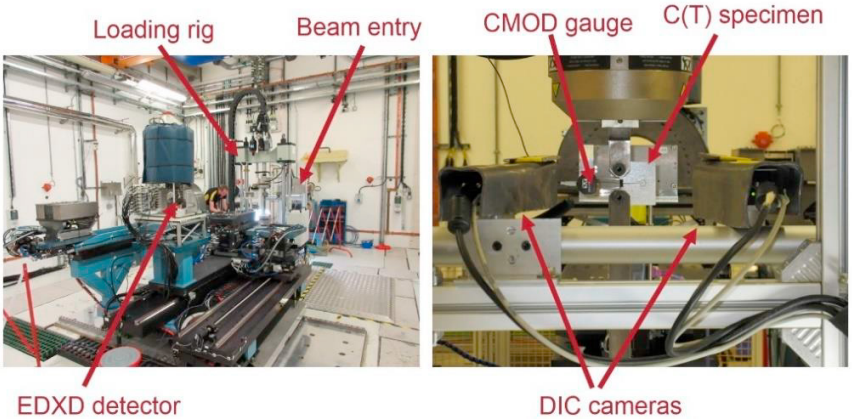

Figure 5: I12 synchrotron beamline set up for Energy Dispersive X-ray Diffraction measurements on a loaded C(T) specimen. Left: overview of the measurement setup. Right: view of the specimen, looking from the direction of the beam entry port.

The measured stress and strain field plots shown in Figure 6 indicate that the strain-hardened region present in the indented specimens affected the stress and strain field which developed during loading of the specimens. In this experiment, the material and specimen configuration favoured an extremely ductile failure mode. This meant that the residual stress introduced by indentation had a negligible effect on the J-integral at the point of tearing initiation. By contrast, due to the greater amount of plasticity which occurs in these specimens prior to tearing initiation, prior strain-hardening affected the failure process much more strongly. This conclusion was supported by the results of FEA (see Figure 7), which showed that although the residual stress caused by indentation initially has a significant effect on the SERR, at the point of tearing initiation the effect of initial strain-hardening dominates. A comparison of 10 indented and 10 non-indented specimens showed that indentation ahead of the crack tip gave an increase in mean load capacity of 0.45 kN (4.2%) and a reduction in mean absorbed energy prior to unstable tearing of 1.45 J (3.2%). This suggests that it may be possible to use non-uniform strain-hardening to tailor the response of a material to its expected fracture mechanism, trading-off load capacity for ductility or vice versa, depending on whether a more brittle or more ductile failure mode is anticipated.

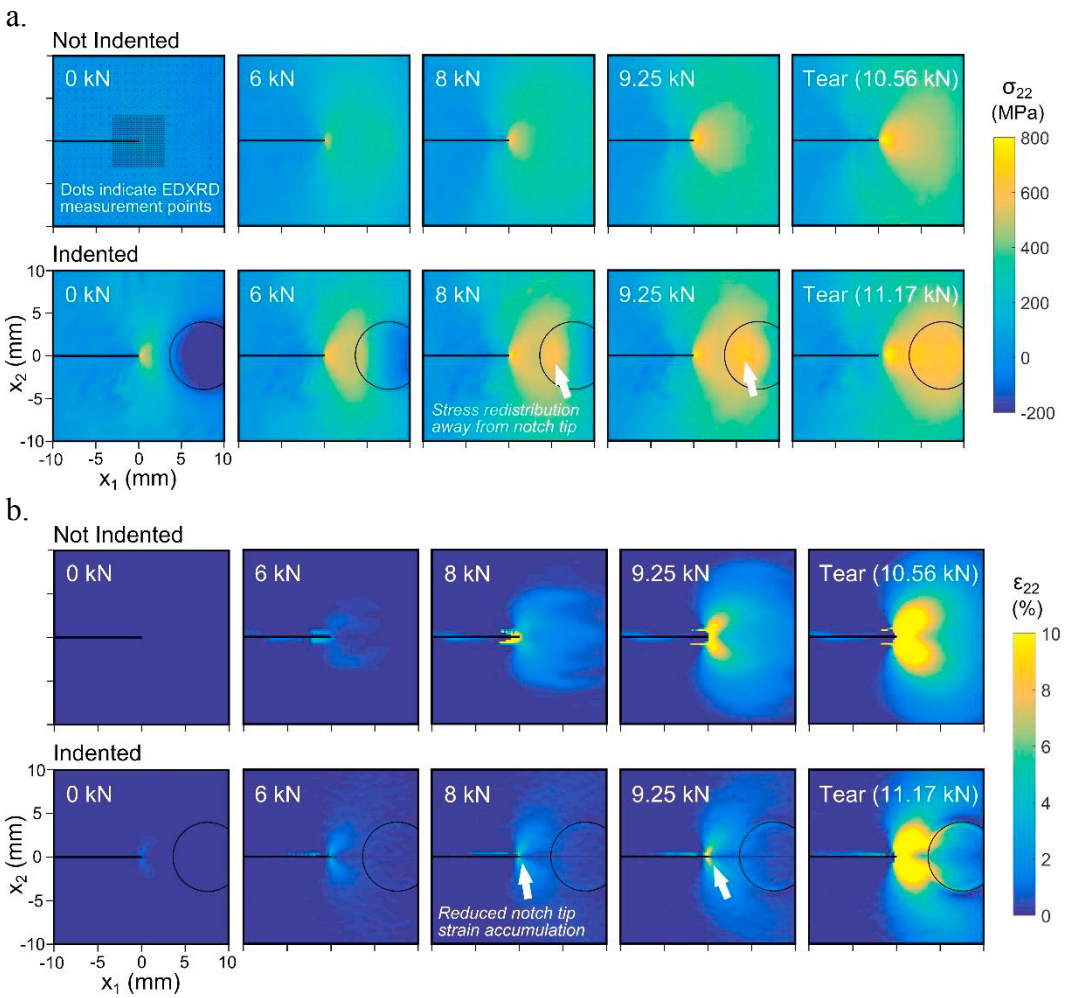

Figure 6: Measured stress (a.) and strain (b.) fields observed around the notch tip of indented and non-indented C(T) specimens of BS 1501-224 28B ferritic steel during loading, from EDXD and DIC measurements. The crack-transverse components (σ_{22} and ε_{22}) only are shown. As in Figure 3, note the presence of residual stress in the indented specimen at zero load in (a.). Circles indicate the indented region.

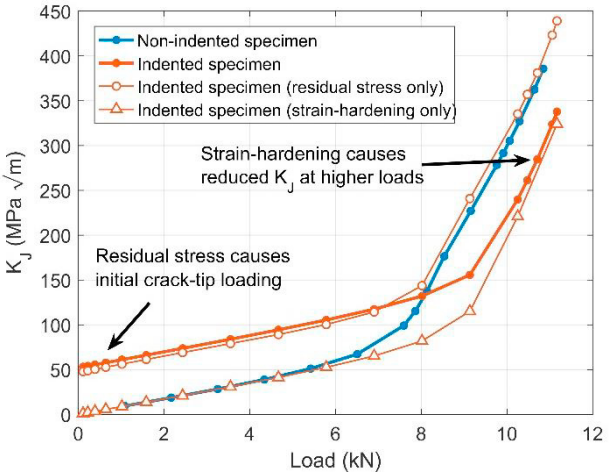

Figure 7: Elastic-plastic equivalent stress intensity factor (K_J) as a function of load, as determined from non-linear FE analyses of indented and non-indented C(T) specimens of BS 1501 224 28B ferritic steel. Additional models of the indented specimen were used to determine the specimen's behaviour if only the residual stress effects or only the strain-hardening effects of indentation were accounted for, demonstrating the dominant effect of prior strain-hardening on the SERR at the point of tearing initiation.

3. Conclusions

The fracture of ductile materials is influenced not only by residual stresses, but also by spatial variations in a material's hardening state that influence the crack tip stress field as loading occurs. These factors affect both fracture initiation and the subsequent propagation of a crack. In the examples shown here, where mechanical indentation was used to introduce an initial stress, both residual stress and initial strain-hardening variations occurred together. However, the different levels of material ductility present in each experiment meant that these two factors affected the failure behavior of AA7475-T7351 and BS 1501 224 28B differently. This demonstrates the need for methods which account for non-uniform material states, both in materials fracture testing and in fracture assessment. A modified form of the J-integral formulation for the Strain Energy Release Rate was shown to be a good predictor of crack advance in both cases, so there is a good outlook for the use of this quantity in fracture assessment.

Data availability statement

Data supporting this work can be downloaded from: https://doi.org/10.5523/bris.2hzzpi1of2n3j2mc3lqs5k2ywe and https://doi.org/10.5523/bris.1t6r34y631zff1zdpq0pih5d17.

Acknowledgements

The authors are grateful to Drs K. A. Abburi Venkata, T. Pirling, M. J. Peel and T. Connolley for their contributions to the work described in this article. Access to radiation scattering facilities was provided by the Institut Laue-Langevin (expt. no. 1-02-185) and the Diamond Light Source (expt. no. EE11463). Funding was provided by the UK EPSRC (grant no. EP/M019446/1 and Impact Acceleration Account).

References

ASTM, 2015, *E561-15a Standard Test Method for KR Curve Determination*, ASTM International, West Conshohocken, PA, USA.

BSi, 2013. *BS 7910:2013+A1 (incorporating corrigenda 2) - Guide to methods for assessing the acceptability of flaws in metallic structures*, BSi.

Budden, P.J. & Sharples, J.K., 2003. Treatment of secondary stresses. In R. A. Ainsworth & K.-H. Schwalbe, eds. *Comprehensive Structural Integrity, Volume 7*. Elsevier-Pergamon, pp. 245–288.

Coules, H.E. et al., 2019. Localised prior strain-hardening increases the tearing resistance of ductile steel. *International Journal of Mechanical Sciences*, 150, pp.103–111.

Coules, H.E. et al., 2018. The effects of residual stress on elastic-plastic fracture propagation and stability. *Materials & Design*, 143, pp.131–140.

Drakopoulos, M. et al., 2015. I12: the Joint Engineering, Environment and Processing (JEEP) beamline at Diamond Light Source. *Journal of Synchrotron Radiation*, 22, pp.828–838.

EDF, 2015. *R6: Assessment of the Integrity of Structures Containing Defects, Revision 4, Amendment 11*, EDF Energy, Gloucester.

Hill, M.R. & VanDalen, J.E., 2008. Evaluation of residual stress corrections to fracture toughness values. *Journal of ASTM International*, 5(8), p.101713.

Lei, Y., 2005. J-integral evaluation for cases involving non-proportional stressing. *Engineering Fracture Mechanics*, 72(4), pp.577–596.

Wilson, W.K. & Yu, I.-W., 1979. The use of the J-integral in thermal stress crack problems. *International Journal of Fracture*, 15(4), pp.377–387.

Withers, P.J., 2007. Residual stress and its role in failure. *Reports on Progress in Physics*, 70(12), pp.2211–2264.